

On-sky Doppler Performance of TOU Optical Very High Resolution Spectrograph for Detecting Low-Mass Planets

Jian Ge, Bo Ma, Sirinrat Sithajan, Michael A. Singer, Scott Powell, Frank Varosi, Bo Zhao, Sidney Schofield, Jian Liu, Nolan Grieves, Anthony Cassette, Louis Avner & Hali Jakeman
Department of Astronomy, University of Florida

Matthew Muterspaugh & Michael Williamson
Center of Excellence in Information Systems, Tennessee State University

Rory Barnes
Department of Astronomy, University of Washington
Email: jge@astro.ufl.edu

The TOU *robotic, compact* very high resolution optical spectrograph ($R=100,000$, 0.38-0.9 microns) has been fully characterized at the 2 meter Automatic Spectroscopy Telescope (AST) at Fairborn Observatory in Arizona during its pilot survey of 12 bright FGK dwarfs in 2015. This instrument has delivered sub m/s Doppler precision for bright reference stars (e.g., 0.7 m/s for Tau Ceti over 60 days) with 5-30 min exposures and 0.7 m/s long-term instrument stability, which is the best performance among all of the known Doppler spectrographs to our knowledge. This performance was achieved by maintaining the instrument in a very high vacuum of 1 micron torr and about 0.5 mK (RMS) long-term temperature stability through an innovative close-loop instrument bench temperature control. It has discovered a 21 Earth-mass planet ($P=43$ days) around a bright K dwarf and confirmed three super-Earth planetary systems, HD 1461, 190360 and HD 219314. This instrument will be used to conduct the Dharma Planet Survey (DPS) in 2016-2019 to monitor ~ 100 nearby very bright FGK dwarfs (most of them brighter than $V=8$) at the dedicated 50-inch Robotic Telescope on Mt. Lemmon. With very high RV precision and high cadence (~ 100 observations per target randomly spread over 450 days), a large number of rocky planets, including possible habitable ones, are expected to be detected. The survey also provides the largest single homogenous high precision RV sample of nearby stars for studying low mass planet populations and constraining various planet formation models. Instrument on-sky performance is summarized.

Key words: Doppler, exoplanets, high cadence, survey, high spectral resolution, optical spectrograph, FGK dwarfs and high precision

1. Introduction

The discovery of the hot Jupiter around 51 Peg in 1995 using Doppler spectroscopy has triggered the start of an intensive era of discoveries of exoplanets. Since the launch of the *Kepler* space satellite in 2009, *Kepler* transit search has made a major breakthrough in identifying thousands of low-mass planet candidates while significantly improving statistical study of the exoplanetary systems¹. To date, a total of 1642 planets have been confirmed while 3787 *Kepler* planet candidates have yet to be confirmed (<http://exoplanets.org>). Transit detections (1147 planets, the majority by *Kepler*) and Doppler techniques (470 planets) contributed the most to these discoveries. Today, the main focus for

future planet surveys is to discover Earth-like planets in habitable zones where life may develop. The Doppler technique will continue to play a key role in this new adventure of identifying low-mass planets and studying planetary system architecture around nearby stars. It also provides a complementary role to space transit missions by measuring planet masses, as transit data can determine planet sizes for most of the planet candidates. The combination of planet mass and size yields clues about the bulky planetary compositions, one of the key parameters to studying planet habitability.

Over the past twenty years, major progress has been made to improve RV precision with Doppler techniques from 3-15 m/s in early 1990's^{2,3,4} to the best long-term RV precision of 0.8 m/s at the present time^{5,6}. The Doppler techniques are mainly based on two instrument calibration approaches, the self-calibration technique using superimposition of an iodine absorption spectrum on stellar spectra³, and the simultaneous calibration technique using a ThAr emission spectrum as a reference⁷. The major advantage of the iodine method is that the instrument point spread functions (PSFs) can be continuously measured to minimize RV measurement uncertainties caused by instrument drifts, but this method has restricted wavelength coverage, ~0.49-0.60 μm , where iodine has strong absorption lines. The major advantage of the simultaneous calibration method is its broad operation wavelength coverage (e.g. 0.38-0.69 μm for HARPS) and throughput gain over the iodine method while the major disadvantage is that the instrument requires very stable environment (pressure and temperature) and spectrograph illumination to minimize the difference between the science and reference beams. The HARPS long-term instrument stability was measured at 1.1 m/s (RMS) over a month^{8,9}. The ThAr lamp aging issue and sparseness of the ThAr emission lines also limit the ThAr simultaneous calibration method to the best calibration precision of ~0.3m/s⁸. After removing the instrument drift using ThAr calibration, HARPS has reached a long-term RV precision of ~0.8 m/s for stellar observations⁶.

What are the major instrument sources affecting the high-precision RV measurements? For HARPS type RV spectrographs using the simultaneous calibration method, instrumental effects include photon noise, instrument drifts, calibration error, spectrograph illumination effects, spectral contamination and stellar jitters. Currently, photon noise is not the dominant source¹⁰. The use of an optical double scrambler, octagonal fibers and a tip-tilt system in both HARPS and HARPS-N has also reduced spectrograph illumination effect to a negligible level^{11,12,13,14}. The combination of instrument long-term drifts (~1.1m/s over one month), ThAr calibration error and stellar jitters has led to ~0.8 m/s RV measurement uncertainties⁶. Recent simulation studies by Dumusque et al.^{15,16} show that stellar jitters can be reduced to ~0.2-0.3 m/s for a solar-type star with stellar activities similar to the Sun by adopting the 3N3 observing strategy, i.e., three measurements per night of 10 min each with 2 hours of spacing, with one visit every three nights for each month. In order to significantly improve RV measurement precision, it is critical to reduce instrument long-term stability.

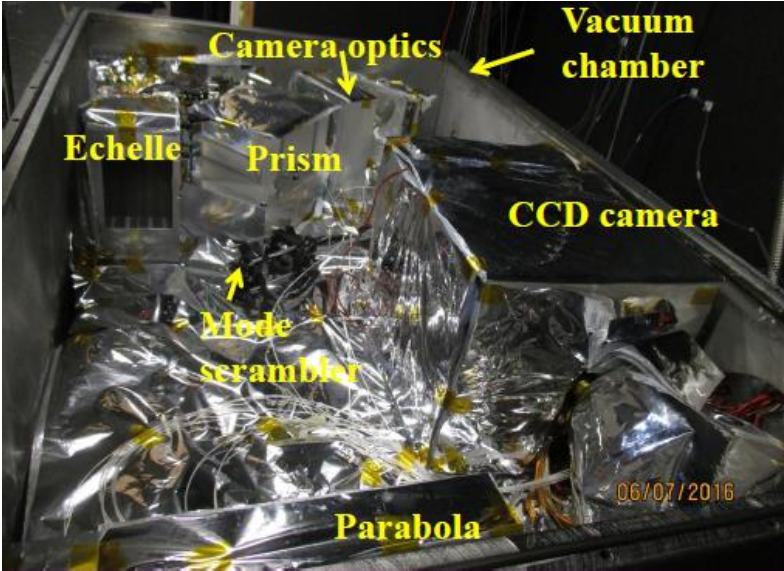


Figure 1.1. The TOU optical high-resolution spectrograph inside a vacuum chamber in a temperature controlled room next to the 50-inch automatic telescope at Mt. Lemmon in Arizona in June 2016. MLI insulation layers are wrapped around mechanical mounts and the spectrograph bench to provide further insulation from the chamber. The bench and the CCD camera mount are temperature controlled by a PID loop.

At the University of Florida, we developed an optical very high-resolution spectrograph, called TOU, with $R=100,000$ and wavelength coverage of $0.38-0.9 \mu\text{m}$ in 2010-2013 (**Figure 1.1**)¹⁷. It is designed for a dedicated low-mass planet survey around nearby FGK dwarfs at the 50-inch automatic telescope at Mt. Lemmon (**Figure 1.2**). Substantial progress has been made in reducing the TOU long-term drifts and developing a data pipeline since commissioning TOU in Arizona in July 2013. After the last major hardware upgrade in September 2015, TOU has reached a stability of ~0.7 m/s (RMS) over one month, 1.5 times smaller than of that achieved with HARPS⁹. Data processing of the stable reference star, Tau Ceti, has already shown an RMS of 0.7 m/s over 60 days, smaller than that (0.92 m/s) obtained by HARPS¹⁸. This instrument will be used to launch the Dharma planet survey in September 2016.

2. The Dharma Planet Survey of Low-mass Planets

The Dharma Planet Survey (DPS) is designed to detect and characterize close-in low-mass planets and sub-Jovian planets at the orbital region (~200-450 days) amenable to future space-imaging missions. The ultimate survey goal is to detect potentially habitable super-Earth planet candidates (**Figure 2.1**) to independently measure η_{\oplus} and provide high priority targets for future space imaging missions (such as WFIRST-AFTA and LUVOIR surveyor) to identify possible biomarkers supporting life¹⁷. It will initially search for and characterize low-mass planets around 100 nearby bright FGK dwarfs (25 late F, 50 G dwarfs, and 25 K dwarfs with $V < 7$ and within ~25 pc, **Figure 2.2**) in 2016-2019, and then continue to monitor targets with linear trends and observe more targets after 2019.

The DPS survey adopts a completely different strategy than previous low-mass planet surveys using ground-based Doppler spectrographs^{19,5}. Instead of surveying a large number of targets with variable number of measurements (from a few RV data points to ~400 RV data points⁶), the DPS survey will offer a homogeneous high cadence for every survey target, i.e. 100 RV measurements randomly spread over 450 days (about one measurement every other night for a typical survey target after excluding the Arizona Monsoon season and bad weather). This includes one set of high-cadence observations on ~10 consecutive observable nights to target short-period low-mass planet detection.



Figure 1.2. The 50-inch fully robotic telescope at Mt. Lemmon in March 2016.

The automatic nature of the 50-inch telescope and its flexible queue observation schedule are key to realizing this homogenous high cadence. This cadence will minimize the time-aliasing in detecting low-mass planets, especially those in highly eccentric orbits, which can be missed by previous surveys. Because of the homogenous cadence for every survey star, both detections and non-detections from the survey can be reliably used for statistical studies. This survey strategy, cadence, and schedule will therefore offer the best accuracy to assess the survey completeness and to determine occurrence rates of low-mass planets. As illustrated in **Figure 2.3**, our survey strategy allows for probing most of the parameter space in the planet mass-period distribution of nearby bright FGK dwarfs to independently verify characteristics (such as distribution, orbital properties, stellar properties, and occurrence rates) of the close-in low-mass planet population identified by the ground-based RV surveys and the *Kepler* mission^{5,21}. It also covers the periods ~200-450 days, which are critical for the upcoming WFIRST-AFTA and LUVOIR direct-imaging missions. This survey will offer a homogeneous data set for constraining formation models of low-mass planets with periods less than 450 days.

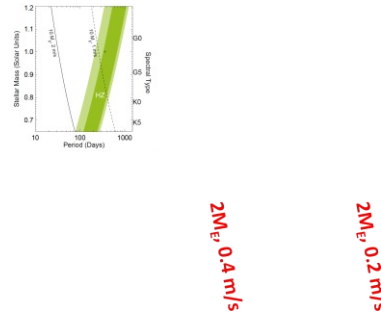


Figure 2.1. The HZ as a function of stellar mass (spectral type) and orbital period, as defined by Kopparapu et al.²⁰. Dark green is a conservative HZ, light green an optimistic extension. Overlaid are contours of stellar reflex velocity due to 2 and 10 Earth-mass planets.

2.1. Survey Target Selection: Our survey targets were selected from the following catalogs: Gliese Catalog of Nearby Stars (Spring 1989); Gliese Catalog of Nearby Stars cross identified with 2MASS²²; ROSAT All-Sky Survey: Nearby Stars²³.

- Spectral type: ~F5V-K7V.
- Brightest stars in each subtype that satisfy the following criteria:
 - o No stellar companions within 5"
 - o $v \sin i < 3$ km/s
 - o RV jitter < 2 m/s (for GK dwarfs, and < 3 m/s for F dwarfs) if available
 - o In active stars, using any available indicators.
 - $\log R'_{HK} < -4.85$
 - ratio between X-ray luminosity and bolometric luminosity, $R_x < -3.0$, if activity level is unknown
 - o < 30 RV observations with better than 3 m/s Doppler precision if observed before
 - o RAs are randomly distributed from 0-360 deg. and DEC's are between -20 and 90 deg.

Figure 2.2 shows magnitude and effective temperature distributions of our selected targets.

2.2. Planet Survey Simulation and Yield: We conducted a survey simulation (including schedule and yield study) to estimate 1) telescope time required to complete the DPS survey 2) The number of expected planet detections from the survey.

To determine the telescope time required to complete the survey, we simulated nightly observation schedules for selected survey targets. Target observable time and seasons, weather, moon effect, daily sunset and sunrise, the Arizona monsoon season (July 1st to Sept. 15th excluded from observations), and target exposure time and telescope slew time (5 min each)

are taken into account. The planned cadence is adopted. Our schedule simulation shows that 92 targets will be observed 100 times while the rest of targets will be observed between 90-98 times by the end of the survey, and only about 58% of the telescope time will be used to complete the planned survey. We adopt exposure times of 10 min, 15 min, and 30 min for $V < 5$, $5 \leq V < 6$ and $6 \leq V \leq 7$ targets, respectively, in the schedule simulation. The exposure time is calculated based on a minimal requirement of $S/N=200$ per pixel at $0.55 \mu\text{m}$ except for $V < 5$ stars which we keep a minimal 10 min exposure for (leading to $S/N > 200$) in order to largely average out stellar P-mode noise⁷.

The photon-limited RV measurement errors to be reached with our targets are estimated from stellar spectrum simulations. High-resolution synthetic optical stellar spectra, generated by the PHOENIX code²⁴, are used for this prediction. TOU instrument parameters (such as the measured overall detection efficiency, wavelength coverage, spectral resolution, resolution sampling, 3.4 pixels, and S/N) were used in spectral synthesis. **Table 2.1** lists photon-limited measurement uncertainties of different spectral type at different stellar rotational velocities.

We simulated RV measurements to derive survey sensitivity and completeness using the simulated target schedule. Two cases of RV performance are used. The optimistic case is based on RV measurement uncertainties from a combination of 1.5 times photon noise (including the pipeline error) of survey targets and wavelength solution (calibration, 0.4 m/s) and other errors dominated by stellar jitters (0.8 m/s), while the pessimistic case includes an additional 2.0 m/s long-term systematic error applied to

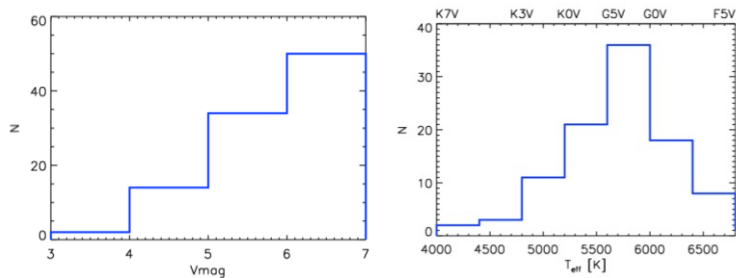


Figure 2.2. (Left). V magnitude distribution of selected stars for the DPS survey. (Right). T_{eff} distribution of the selected survey targets.

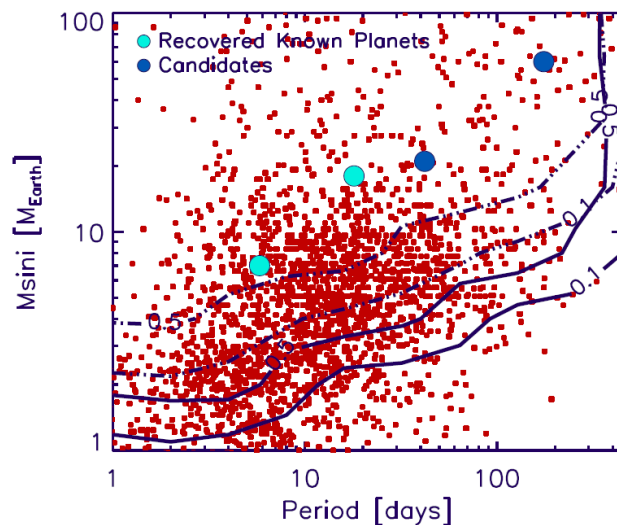


Figure 2.3. The predicted contours (10% and 50%) of the DPS survey completeness (the solid blue). Red dots are Kepler planet candidates from NASA Exoplanet Archive website. Masses of *Kepler* planet candidates are derived from the mass-radius relations by Lissauer et al.²⁵. Two confirmed super-Earths (big cyan dots) and two new candidates (big blue dot) identified by the DPS pilot survey are also marked on the plot.

uncertainties from a combination of 1.5 times photon noise (including the pipeline error) of survey targets and wavelength solution (calibration, 0.4 m/s) and other errors dominated by stellar jitters (0.8 m/s), while the pessimistic case includes an additional 2.0 m/s long-term systematic error applied to

all survey targets. Previous simulations by Dumusque et al.^{15,16} show that binning of RV measurements in sequence over 10 days can significantly reduce stellar jitters from ~2 m/s down to ~0.8 m/s. Given that the majority of our targets have a stellar jitter level < 2 m/s, we expect the final jitter induced RV uncertainties to be within 0.8 m/s for at least some of the survey targets after the binning method is adopted in RV measurements. Our pessimistic consideration represents possible RV performance for a survey star without significant reduction of stellar activity induced RV jitters, or F dwarfs, some of which have jitters at 2-3 m/s after binning is used.

The predicted planet yields, including habitable super-Earth and Neptune candidates, are listed in **Table 2.2** for FGK dwarfs from both the optimistic and pessimistic cases. We adopted the occurrence rates for P=250-450d, we assume the flat rate in the logP space for FGK dwarfs^{27,28}. The definition of Earth-size, super-Earths, Neptunes and sub-Jovian planets are adopted here: Earth-size (0.8-1.2 R_⊕, or 0.7-1.4M_⊕,

Table 2.1. Photon-limited RV measurement errors for FGK dwarfs with S/N =200 per pixel at 0.55 μm with TOU.

<i>vsini</i> /Spec. type	F5V	G0V	G5V	K0V	K5V
0 km/s	0.30 m/s	0.25 m/s	0.21 m/s	0.19 m/s	0.14 m/s
2 km/s	0.34 m/s	0.28 m/s	0.25 m/s	0.22 m/s	0.20 m/s
5 km/s	0.55 m/s	0.46 m/s	0.41 m/s	0.38 m/s	0.36 m/s

Table 2.2. Predicted DPS planet yields around FGK dwarfs

Case	Super-Earths	Neptunes	Sub-Jovians	Habitable super-Earths	Habitable Neptunes
Optimistic(overall)	11(±9%)	26(±4%)	6(±14%)	2 (±70%)	4 (±25%)
Pessimistic(overall)	2(±63%)	20(±5%)	6(±15%)		2 (±65%)
Optimistic (F)	1	4(±24%)	1		
Pessimistic (F)		3(±33%)	1		
Optimistic (G)	5(±20%)	14(±7%)	4(±24%)	1	2 (±66%)
Pessimistic (G)	1	11(±9%)	4(±26%)		1
Optimistic (K)	5(±20%)	8(±13%)	1	1	2 (±63%)
Pessimistic (K)	1	6(±16%)	1		1

the mass-radius relationship is from Lissauer et al.²⁶), super-Earth (1.2-2.3 R_⊕, or 1.4-5.7M_⊕), Neptune (2.3-5.7R_⊕, or 5.7-36M_⊕) and sub-Jovian planet (5.7-11R_⊕, or 36-128M_⊕). The large systematic measurement errors of 2 m/s applied to all of the survey stars in the pessimistic case have a major effect on the detection sensitivity for super-Earths while it does not significantly affect the detection of Neptunes and sub-Jovian planets.

Figure 2.3 shows survey detection sensitivity and completeness levels from both the optimistic and pessimistic cases. It is quite interesting to see that our high cadence survey can probe most of the close-in low-mass planet population in the mass-period space identified by *Kepler*. The survey completeness has largely been improved over the HARPS FGK dwarf survey. For instance, about 50% of planets with ~6 M_⊕ and P~100 days can be detected under the optimistic case and ~50% of planets with ~10 M_⊕ and P~100 days can be detected under the pessimistic case. Our optimistic detections can provide sensitive measurements of planet occurrence rates for super-Earths, Neptunes, and sub-Jovian planets, while pessimistic detections can still provide meaningful measurements of planet occurrence rates for these planets with orbital periods of up to 450 days, which was not measured by previous RV surveys. In addition to providing sensitive measurements of planet occurrence rates for

super-Earths, Neptunes, sub-Jovian planets, DPS is likely to detect a few habitable super-Earth and Neptunes around nearby GK dwarfs.

3. DPS Survey Spectrograph and Pilot Survey Performance

The TOU optical cross-dispersed echelle spectrograph adopts the HARPS design but with several design refinements to significantly reduce its volume and construction cost while substantially increasing its wavelength coverage (by a factor of 1.7, **Figure 3.1**, 0.38-0.9 μm vs. 0.38-0.69 μm in HARPS⁷). It also maintains a similar spectral resolution ($R=100,000$ vs. $R=115,000$) and spectral sampling (3.4 pixels) to HARPS^{29,30,17}. The extra wavelength coverage at 0.69-0.9 μm compared to HARPS would benefit RV measurements for K dwarfs, which have a peak flux around 0.7 μm . Like HARPS, TOU is operated in a vacuum chamber, but TOU's vacuum is kept at a much lower pressure: it is kept under 0.01mTorr through continuous pumping by a turbo pump while HARPS's vacuum is kept at ~ 7.5 mTorr⁷. This kind of low vacuum level has helped minimize the pressure effect on temperature control.

TOU's temperature has been extremely carefully controlled through four layers of insulation and year-round temperature control. An air-conditioned (A/C) instrument room provides the first layer of temperature control and is kept at 16.7(± 0.2) $^{\circ}\text{C}$. A compartment inside the A/C room provides the second layer of temperature control. Its temperature is set at 21.4 $^{\circ}\text{C}$ and controlled by a PID loop to within ± 50 mK. A thermal enclosure provides the third layer of insulation. Its temperature is controlled by another PID loop and keep the chamber walls within ± 1 mK of a setting point (24 $^{\circ}\text{C}$). The last layer of insulation is provided by Multi-layer insulation (MLI) wrapped around the spectrograph bench and mechanical mounts. The bench and the CCD mount temperatures are further controlled by a closed-loop temperature control to within ± 1 mK (RMS=0.5 mK). This closed-loop bench control has eventually helped us reach ~ 0.7 m/s (RMS) long-term RV stability (over a month) without calibration as shown in **Figure 3.2**.

Like HARPS, TOU adopts the ThAr calibration method. Its short-term instrument drift is calibrated by a ThAr emission lamp, called an operational ThAr source, while the long-term stability

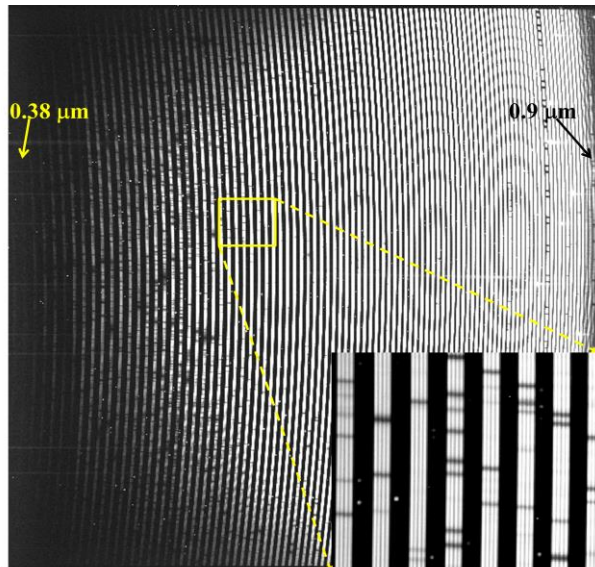


Figure 3.1. A stellar spectrum of Tau Ceti in 5 min exposure with TOU at $R=100K$. The ThAr calibration spectrum can be seen in the zoom-in spectrum. Stellar spectrum is nearly completely covered in a single exposure.

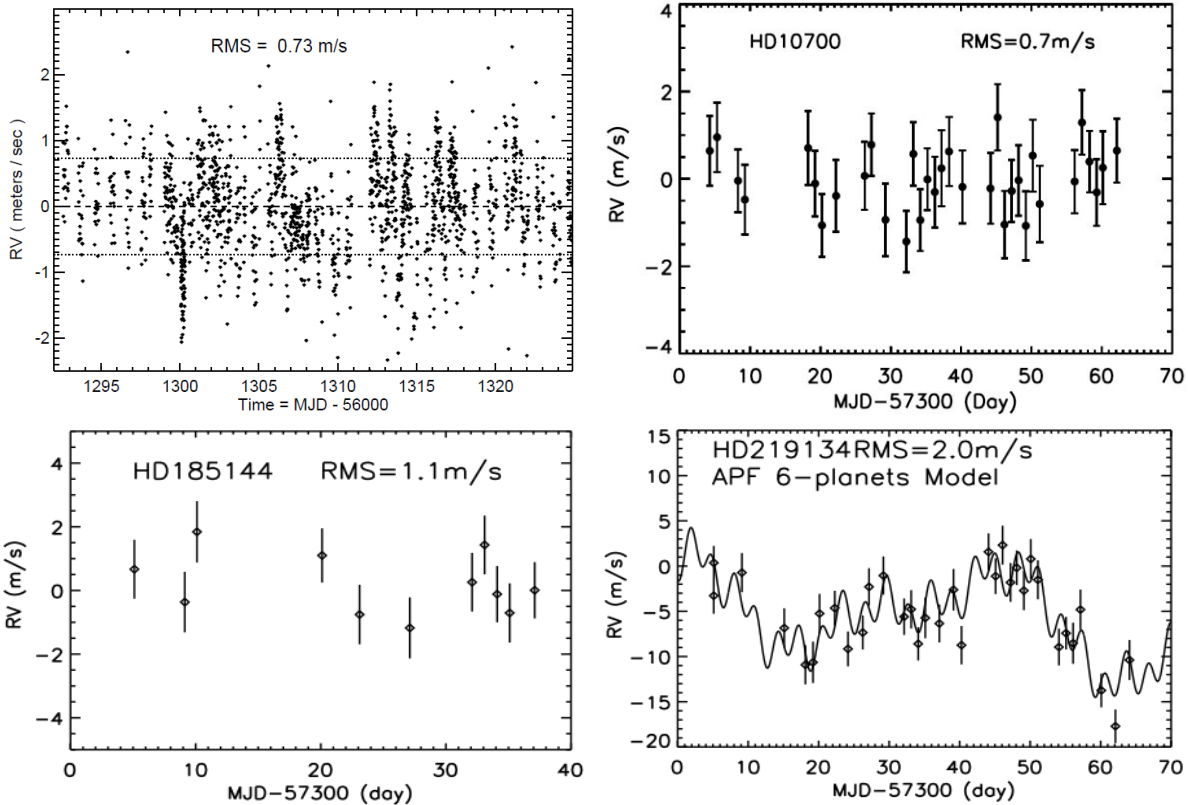


Figure 3.2. RVs after a major hardware upgrade in September 2015. From Top Left to Bottom Right: (a). TOU instrument drift measurements (RMS=0.73 m/s) over 33 days tracked with ThAr spectra. (b). RVs of a stable star, Tau Ceti over 62 days. RMS=0.7m/s. (c). RVs of a stable star, HD 185144 over 32 days. RMS=1.1 m/s. (d). RVs of a multiple planet system around HD 219314. The solid line is the predicted RV from six planets detected by Vogt et al.³¹.

is calibrated by a master ThAr lamp, called a reference ThAr source. The master lamp is only turned on once per day to sustain its lifetime for multiple years to provide long-term instrument offset calibration. Our current ThAr data processing pipeline has achieved 0.21 m/s instrument drift calibration precision over a long term (~60 days). **Figure 3.3** shows an example of instrument drift over two days (RMS =0.55 m/s and P-V~2 m/s) and its corresponding calibration precision (0.21 m/s) after the low frequency daily small drift is removed. This calibration precision is slightly better than that produced by HARPS, which is ~0.3 m/s⁸.

The Pilot Survey Performance: A total of 12 nearby FGK dwarfs were monitored in the pilot survey in 2015. Most of the data have been processed. **Figure 3.4** shows a histogram of RMS of RVs of survey targets including four RV stable stars, three new stars without clear planet signals, and residuals of five targets with the planet signals removed. Compared to previous low-mass planet surveys (HARPS⁵; the Eta-Earth Survey¹⁹), our mean RMS (1.8 m/s) is between the survey performance of HARPS (1.4 m/s, Mayor et al. 2011) and the Eta-Earth Survey (~2.5 m/s¹⁹). **Figure 3.2** shows RV measurements of two RV stable stars (Tau Ceti and HD 185144) and one known planet system (HD 219134). **Figure 3.5** shows RV measurement performance of four survey stars: two RV stable stars (HD 9407 and HD 22484) and two known planet host stars (HD 1461b and HD 190360b). The RMS for RV measurements of the stable star Tau Ceti over ~60 days is 0.7 m/s, which is better than that (0.92 m/s) reported by HARPS¹⁸. The measurements of HD 185144 show an RMS error of 1.1 m/s over 32 days, better than the 1.5 m/s RMS measured by Keck HIRES and Lick Automated Planet Finder (APF)³². RVs of HD 219134 in our data show clear variation. Due to the limited 32 RV points over 62 days, it is hard to separate all of the possible planet signals from this system. Instead, we over-plotted predicted RV curve from six planets reported in Vogt et al.³¹ and found that our data are quite consistent with the prediction.

The RMS of the RV residual after the planet signals are subtracted is 2.0 m/s, which is also consistent with the RMS of 1.8 m/s obtained with the APF measurements and 2.5 m/s with the Keck HIRES measurements³¹. An RMS for the stable star HD 9407 (V=6.5) of 1.7 m/s (dominated by photon noise) over ~60 days is consistent with that (1.6 m/s) measured with Keck HIRES^{33,32}. The RV residuals for two confirmed super-Earths, HD 190360c³⁴ and HD 1461b³⁵, are also consistent with that reported in the original discovery papers. Two strong planet candidates (DPS-1b and DPS-2b) have been identified among five new-search stars. DPS-1b is a Neptune candidate around a bright K dwarf (Msini=21M_⊕, P=43d, e=0.33) while DPS-2b is a sub-Jovian planet candidate around an F dwarf (Msini=0.19 M_J, P=175d, e=0.23). Details about the RV measurements of these two candidates will be reported in an ApJ paper (Ge et al. 2016 in preparation). Most of the pilot targets have ~1-2 m/s RMS, which likely results from stellar activity jitters. All of the pilot observation performance indicates that TOU is ready for the Dharma Planet Survey in the fall of 2016.

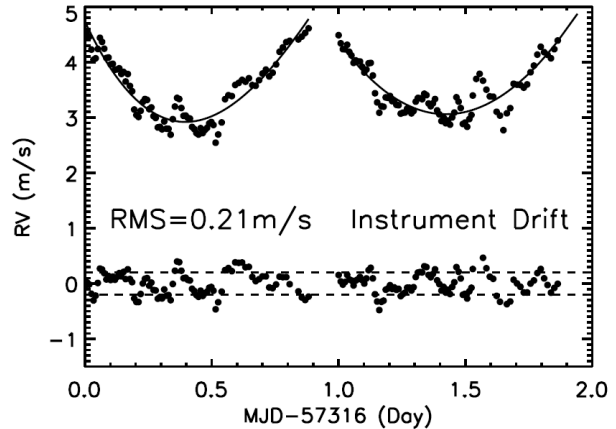


Figure 3.3. ThAr measurements over two nights with RMS=0.55 m/s (Top). 0.21 m/s calibration accuracy has been reached after the low frequency instrument drift component (the solid line fitting) is removed.

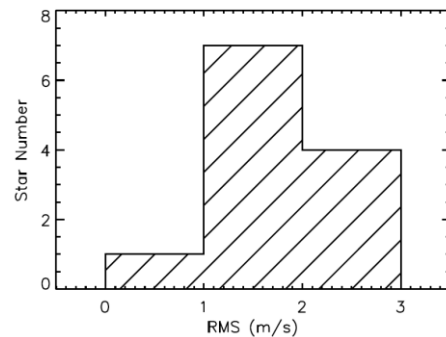


Figure 3.4. Histogram of the RMS of the RV measurements of the DPS survey stars. Planet signals have been removed from the five survey targets.

Acknowledgment: This work has been supported by Dharma Endowment Foundation, DoD Cooperative Agreement W911NF-09-2-0017, the W.M. Keck Foundation, NSF-PAARE grant 1059158, state of Tennessee through its Centers of Excellence program and the University of Florida.

REFERENCES

1. Borucki, W. et al. "KEPLER: Search for Earth-Size Planets in the Habitable Zone." IAUS, 253, 289–299 (2009).
2. Walker, G. et al. "Gamma Cephei - Rotation or planetary companion?" ApJ, 396, 91 (1992).
3. Butler, R. P. et al. "Attaining Doppler Precision of 3 M s⁻¹." PASP, 108, 500 (1996).
4. Baranne, A. et al. "ELODIE: A spectrograph for accurate radial velocity measurements." A&AS, 119, 373–390 (1996).
5. Mayor, M., et al. "The HARPS search for southern extra-solar planets XXXIV. Occurrence, mass distribution and orbital properties of super-Earths and Neptune-mass planets," arXiv:1109.2497 (2011).
6. Dumusque, X., Pepe, F., Lovis, C., Ségransan, D., Sahlmann, J., Benz, W., Bouchy, F., Mayor, M., Queloz, D., Santos, N., Udry, S., "An Earth-mass planet orbiting alpha Centauri B," Nature, 491, 207 (2012).
7. Mayor, M. et al. "Setting New Standards with HARPS," Messenger, 20, 114 (2003).
8. Lovis, C. & Pepe, F. "A new list of thorium and argon spectral lines in the visible," A&A, 468, 1115 (2007).
9. Pepe, F. "From HARPS/HARPS-N to ESPRESSO: pushing the limits further," Astronomy of Exoplanets with Precise Radial Velocities, held August 16-19, 2010 Penn State University University Park, PA, USA. Online at <http://exoplanets.astro.psu.edu/workshop>, id.17 (2010).
10. Lovis, C. et al. "An extrasolar planetary system with three Neptune-mass planets," Nature, 441, 305 (2006)
11. Avila, G. & Singh, P. "Optical fiber scrambling and light pipes for high accuracy radial velocities measurements." in Astronomical Telescopes and Instrumentation: Synergies Between Ground and Space (Atad-Ettedgui, E. & Lemke, D.), SPIE, 7018, 70184W–70184W–7 (2008).
12. Chazelas, B., Pepe, F. & Wildi, F. "Optical fibers for precise radial velocities: an update." in SPIE Astronomical Telescopes + Instrumentation (Navarro, R., Cunningham, C. R. & Prieto, E.) 8450, 845013 (2012).
13. Cosentino, R. et al. Harps-N: the new planet hunter at TNG. in SPIE Astronomical Telescopes + Instrumentation (McLean, I. S., Ramsay, S. K. & Takami, H.) 8446, 84461V (2012).
14. Cosentino, R. et al. "HARPS-N @ TNG, two year harvesting data: performances and results," Proc. 9147, 8 (2014).
15. Dumusque, X., et al., "Planetary detection limits taking into account stellar noise. I. Observational strategies to reduce stellar oscillation and granulation effects," A&A, 525, 140 (2011).
16. Dumusque, X., Santos, N. C., Udry, S., Lovis, C. & Bonfils, X. "Planetary detection limits taking into account stellar noise. II. Effect of stellar spot groups on radial-velocities," A&A, 527, 82 (2011).
17. Ge, J. et al. "A robotic, compact, and extremely high resolution optical spectrograph for a close-in super-Earth survey," Proc. SPIE, 9147E, 86G (2014).
18. Pepe, F. et al. "The HARPS search for Earth-like planets in the habitable zone. I. Very low-mass planets around HD 20794, HD 85512, and HD 192310," A&A, 534, 58 (2011).

19. Howard, A., Marcy, G., Johnson, J., Fischer, D., Wright, J., Isaacson, H., Valenti, J., Anderson, J., Lin, D., Ida, S. "The Occurrence and Mass Distribution of Close-in Super-Earths, Neptunes, and Jupiters, *Science*, 330, 653 (2010).
20. Kopparapu, R., Ramirez, R., Kasting, J. F., Eymet, V., Robinson, T., Mahadevan, S., Terrien, R., Domagal-Goldman, S., Meadows, V., Deshpande, R. "Habitable Zones around Main-sequence Stars: New Estimates," *ApJ*, 765, 131 (2013).
21. Batalha, N. et al. "Planetary Candidates Observed by Kepler. III. Analysis of the First 16 Months of Data," *ApJS*, 204, 24 (2013).
22. Stauffer, J. et al. "Accurate Coordinates and 2MASS Cross Identifications for (Almost) All Gliese Catalog Star," *PASP*, 122, 885 (2010).
23. Hünsch, M., Schmitt, J. H. M. M., Sterzik, M. F., Voges, W. "The ROSAT all-sky survey catalogue of the nearby stars," *A&AS*, 135, 319 (1999).
24. Husser, T.-O. et al. "A new extensive library of PHOENIX stellar atmospheres and synthetic spectra," *A&A*, 553, 6 (2013).
25. Mulders, Gijs D.; Pascucci, Ilaria; Apai, Dániel, "A Stellar-mass-dependent Drop in Planet Occurrence Rates," *ApJ*, 798, 112 (2015)
26. Lissauer, J. et al., "Architecture and Dynamics of Kepler's Candidate Multiple Transiting Planet Systems," *ApJS*, 197, 8 (2011).
27. Dong, S.B. & Zhu, Z.H. "Fast Rise of "Neptune-size" Planets ($4-8 R_{\oplus}$) from $P \sim 10$ to ~ 250 Days—Statistics of Kepler Planet Candidates up to ~ 0.75 AU," *ApJ*, 778, 53 (2013).
28. Marcy, G.W., Weiss, L.M., Petigura, E.A., Isaacson, H., Howard, A.W., & Buchhave, L.A., "Occurrence and core-envelope structure of 1-4x Earth-size planets around Sun-like stars," *PNAS*, 11112655 (2014).
29. Ge, J. et al. "Design and performance of a new generation, compact, low cost, very high Doppler precision and resolution optical spectrograph," *Proc. SPIE*, 8446, 30G (2012)
30. Zhao, B. & Ge, J. "Optical design of new generation compact, high resolution and high Doppler precision optical spectrograph," *SPIE*, 8446, 84 (2012)
31. Vogt, S. et al., "A Six-Planet System Orbiting HD 219134," *ApJ*, 814, 12 (2015)
32. Vogt, S. et al. "APF-The Lick Observatory Automated Planet Finder," *PASP*, 126, 359 (2014)
33. Howard, A. et al., "The NASA-UC Eta-Earth Program. II. A Planet Orbiting HD 156668 with a Minimum Mass of Four Earth Masses," *ApJ*, 726, 73 (2011)
34. Wright, J., et al. "Ten New and Updated Multiplanet Systems and a Survey of Exoplanetary Systems," *ApJS*, 693, 1084 (2009)
35. Rivera, E. et al. 2010, "A Super-Earth Orbiting the Nearby Sun-like Star HD 1461," *ApJ*, 708, 1492